Experimental wireless communication using chaotic baseband waveform

Journal:	*IEEE Transactions on Vehicular Technology*
Manuscript ID	Draft
Suggested Category:	Regular Paper
Date Submitted by the Author:	n/a
Complete List of Authors:	Yao, Jun-Liang; Xi'an University of Technology Sun, Yu-Zhe; Xi'an University of Technology Ren, Hai-Peng; Xi'an University of Technology, Grebogi, Celso; University of Aberdeen
Keywords:	Chaos, Wireless communication

Experimental wireless communication using chaotic baseband waveform

Junliang Yao*, Yuzhe Sun*, Haipeng Ren* and Celso Grebogi†

*Shaanxi Key Laboratory of Complex System Control and Intelligent Information Processing, Xi'an University of Technology, Xi'an, P. R. China

†Institute for Complex System and Mathematical Biology, University of Aberdeen, Aberdeen AB24 3UE, United Kingdom

Abstract

Some new properties of the chaotic signal have been used in communication systems recently. They include: (i) chaos is proven to be the optimal communication waveform in the sense of very simple match filter being used to achieve maximum signal to noise ratio; (ii) the amount of information contained in a chaotic signal is unaltered after wireless multipath propagation; and (iii) a chaotic property can be used to resist multipath effect. All these support the application of chaos in a practical communication system. However, due to the broadband property of the chaotic signal, it is very difficult for a practical transducer or antenna to convert such a broadband signal into a signal that would be suitable for practical channel transmission. Thus, the use of chaotic signal properties to improve the performance of conventional communication system without changing the system configuration becomes a critical issue in communication with chaos. In this paper, chaotic baseband signal is used to show that this difficulty can be overcome. A continuous-time chaotic waveform is proven to be topologically conjugate to a symbolic sequence, allowing the encoding of information into the chaotic signal. A finite impulse response filter is used to replace the impulse control in order to encode information into the chaotic signal, simplifying the algorithm for high speed communication. Based on this, a wireless communication system is designed using the chaotic signal as the baseband waveform, which is compatible with the general wireless communication platform. In such a way, the simple matched filter and decoding method, using chaos properties, enhance the communication

system performance. The Bit Error Rate (BER) performance of the proposed wireless communication system is analyzed and compared with the conventional non-chaotic baseband waveform. The results show that the proposed chaotic baseband waveform communication method has better BER performance in both the static and time-varying wireless channel. The experimental results, based on the commonly-used wireless open-access research platform, show that the BER of the proposed method is superior to the conventional method under the real wireless multipath channel.

Index Terms

Experimental wireless communication, multipath channel, chaos, basis function, wireless open-access research platform.

I. Introduction

As an important issue in nonlinear science, chaos has been found in many traditional fields, such as weather forecast, biomedicine, and control systems. Owing to some of its intrinsical properties, chaos has attracted lots of attentions also in the communication fields [1]–[4].

Chaos has been used as a carrier waveform or spread spectrum waveform in dealing with issues such as chaotic masking [5], Chaos Shift Keying (CSK) [6], [7], and Chaos-based Direct sequence Code Division Multiple Access (CD-CDMA) [8]. In these applications, the chaotic waveform does not contain information, instead, the information is masked in the chaotic signal (for chaotic masking) or information is encoded using the key shift (for CSK). At the receiver, the complicated synchronization is usually needed to recover the information. To overcome the synchronization problem, several differential CSKs (DCSKs) [9]–[12] were developed. Another chaotic communication scheme is to encode the message in the chaotic waveform itself by controlling the dynamics of the chaotic system [13]. At the receiver, the message can be decoded with a proper symbolic partition, including the removal of noise by using the chaos property [14], [15]. But there are some encoding constraints in the chaotic attractor [13]. By using a hybrid chaotic system and impulse control, arbitrary message can be encoded [16], [17].

Chaotic communication has been extensively investigated for more than twenty-five years since chaotic synchronization was proposed in [18]. In practice, chaos was reported to be successfully used in an

commercial optical fiber communication system to get higher bit transmission rate [19]. But in other communication media, especially the practical wireless channel, there are few application examples of communication using chaos in the existing literature. The main reasons lie in three aspects: firstly, the chaotic carriers have wide frequency spectrum, so they are not suitable for band-limited wireless channel and, in addition, the traditional Radio-Frequency (RF) antennas cannot be used to transmit chaotic carrier signals; secondly, the chaotic synchronization between the transmitter and the receiver is difficult to be achieved under a multipath time-varying channel, since it increases the system computation complexity to decode information; thirdly, the generation of chaotic signals using the impulse control [16] requires complicated hardware and software support.

To address these three issues for chaos-based wireless communications, we propose in this paper the use of chaos as the baseband waveform and a sinusoidal signal as the carrier waveform. The generation of a chaotic waveform having low complexity is the priority. A method for constructing a continuous-time chaotic waveform was proposed by using linear superposition of special basis function [20]; the sufficient conditions for the basis function ensured that the continuous-time waveform was topologically conjugate to the symbolic dynamics (message) [21]. However, the proposed basis function contains an infinitely long and exponentially increasing oscillations, which is non-causal and impractical to be realized. A hybrid chaotic system and its implemented circuit were proposed in [22]; the output waveform had positive Lyapunov exponents and could be treated as a linear convolution of a symbol sequence and a fixed basis function. The corresponding matched filter could be used to avoid the complicated chaotic system synchronization between the transmitter and the receiver. For wireless communication using chaos, theoretical analyses have shown that the topological entropy of the hybrid chaotic system is unaffected by the wireless multipath propagation [17]. The decoding method using a chaotic property was proposed in [23], which showed reasonable multipath resistance under the time-varying multipath channel. However, the chaotic signal generated by the hybrid chaotic system cannot be used directly in practiced wireless channels because of limited bandwidth [24] in the conventional wireless communication systems. To address this problem, the idea of using the chaotic signal as communication baseband signal was proposed

in [25], and a radio-wave wireless communication system with chaos was built based on the channel simulator.

The results in [25] suggested a simple laboratory demonstration for the wireless communication with chaos, but the theoretical basis of the chaotic encoding and the realization process of the field experiment have not been undertaken so far. In this work, a wireless communication system using the chaotic baseband waveform is being proposed. Firstly, the chaotic waveform, generated from the hybrid dynamical system [22], is proved to be topologically conjugate to the symbolic dynamics, thus the symbol sequence (information) is decodable from the chaotic waveform. Secondly, a chaotic shaping filter is being proposed by using a Finite Impulse Response (FIR) filter to encode information into the chaotic waveform. At the receiver, the matched filter corresponding to the chaotic waveform is used to maximize the Signal-to-Noise Ratio (SNR), and the method in [23] is used to relieve the Inter-Symbol Interference (ISI). Finally, experimental tests are carried out using the Wireless open-Access Research Platform (WARP) for the practical wireless channel. The contributions of this paper are summarized as follows.

1) The chaotic signal is used as communication baseband waveform and the sinusoidal signal is used as the carrier waveform. Comparing with the traditional chaotic carrier communication methods, the occupied bandwidth is narrower and suitable for the band-limited wireless communication applications, e.g., WiFi communication, which avoids the main obstacle of applying chaos in a wireless channel.
2) The chaotic baseband waveform in our method is constructed by the convolution of the basis function with given symbolic stream (information), which is implemented by using an FIR filter. This encoding method is compatible with the conventional communication system, without having the complicated hardware and software support as compared with the impulse control method [16].
3) At the receiver, the matched filter corresponding to the chaotic waveform is used to maximize the SNR, which avoids the complicated chaotic system synchronization between the transmitter and the receiver. The filter output signal and the threshold determined by using a chaotic property are employed to decode information, which relieves the multipath effects without the traditional

complicated channel equalization, and it achieves better BER performance as compared to the traditional method even with the equalization.

4) Both encoding and decoding algorithms are compatible with the traditional system. The proposed chaos-based communication is easily implemented in the universal wireless communication platform, improving the performance without modification to the hardware configuration.

This paper is organized as follows. The proof of the topological conjugation between the chaotic waveform and the symbol sequence is given in Sec. II. The encoding and decoding algorithms of the proposed method are explained in detail in Sec. III. The theoretical performance of the proposed method is analyzed in Sec. IV. Experimental performances of both the proposed method and the conventional non-chaotic method are evaluated in Sec. V. Finally, some conclusions are given in Sec. VI.

II. Topological Conjugation between the Chaotic Waveform and the Symbol Sequence

A hybrid dynamical system [22] given by

$$\ddot{x} - 2\beta\dot{x} + (\omega^2 + \beta^2)x = (\omega^2 + \beta^2)s(t) \tag{1}$$

generates chaotic signal, $x(t)$ [16], [22], and the parameters $\omega = 2\pi$ and $0 < \beta \leq \ln 2$. $s(t) = \mathrm{sgn}(x(t))$ switches its value when $\dot{x}(t) = 0$, keeping its value at other times, The chaotic signal has exact analytic solution given by

$$x(t) = \sum_{m=-\infty}^{\infty} s_m \cdot p(t-m), \tag{2}$$

where s_m is the bi-polar information symbol. $p(t)$ in Eq. (2) is the basis function given by

$$p(t) = \begin{cases} (1-e^{-\beta})e^{\beta t}(\cos\omega t - \dfrac{\beta}{\omega}\sin\omega t), & (t < 0) \\ 1 - e^{\beta(t-1)}(\cos\omega t - \dfrac{\beta}{\omega}\sin\omega t), & (0 \leq t < 1) \\ 0, & (t \geq 1), \end{cases} \tag{3}$$

For communication systems, the information symbols can be recovered from the received signals only if the encoding baseband waveform and the symbol sequence are topologically conjugate [20], [21]. By

defining $\phi_m(t) = s_m{\cdot}p(t-m)$, Eq. (2) can be rewritten as

$$x(t) = \sum_{m=-\infty}^{\infty} s_m{\cdot}p(t-m) = \sum_{m=-\infty}^{\infty} \phi_m(t). \tag{4}$$

The sufficient conditions for the topological conjugation between chaotic waveform $x(t)$ and driving symbols s_m $(m = -\infty, \cdots, \infty)$ are give in [21] as

1) $\phi_k(t) \neq \phi_j(t)$ almost everywhere for $k \neq j$,

2) $\max\limits_{k,j} |\phi_k(t) - \phi_j(t)| < G \cdot 2^{-|t|}$, where $G \in \mathbb{R}$,

3) $\min\limits_{k\neq j} \int_{0\leq t<1} |\phi_k(t) - \phi_j(t)|\mathrm{d}t > \int_{t<0} \max\limits_{k,j} |\phi_k(t) - \phi_j(t)|\mathrm{d}t$.

Under the assumptions of $s_m \in \{-1, 1\}$ and $\beta = \ln 2$, the above conditions are satisfied. The proof is as follows:

For condition 1), $\phi_k(t) \neq \phi_j(t)$ for $k \neq j$ is satisfied, because $|p(t-k)| \neq |p(t-j)|$ when $s_k \in \{-1, 1\}$, $s_j \in \{-1, 1\}$.

For condition 2), we have

$$\begin{aligned} &\max_{k,j} |\phi_k(t) - \phi_j(t)| \\ =&\max_{k,j} |s_k \cdot p(t-k) - s_j \cdot p(t-j)| \\ \leq& 2 \cdot |p(t)| \\ <& 5 \cdot (e^{\beta})^{-|t|}. \end{aligned} \tag{5}$$

Then the condition 2) is satisfied when $G \geq 5$ and $\beta = \ln 2$.

For condition 3), the inequality is satisfied for $\beta = \ln 2$, because

$$\begin{cases} \min\limits_{k\neq j} \int_{0\leq t<1} |\phi_k(t) - \phi_j(t)|\mathrm{d}t = 2\int_{0\leq t<1} |p(t)|\mathrm{d}t \approx 2.4312 \\ \int_{t<0} \max\limits_{k,j} |\phi_k(t) - \phi_j(t)|\mathrm{d}t = 2\int_{t<0} |p(t)|\mathrm{d}t \approx 0.4642. \end{cases} \tag{6}$$

The significance of the topological conjugation lies in that that we cannot only construct the chaotic waveform from the symbol sequence, but also recover the symbol sequence from the chaotic waveform conversely. The chaotic waveform generation using this method (given by Eq. (4)) has been proved to be a forward-time chaos [22], whose topological entropy is unaffected by the wireless multipath channel [17]. These results are very important for the use of chaos in wireless communication, because they imply

that there is no loss of information during the waveform generation and transmission. Thus, in theory, we can completely recover the driving symbols (information) at the receiver using proper methods.

III. Wireless communication system using the chaotic baseband waveform

In order to be compatible with the traditional non-chaotic systems, the Software Defined Radio (SDR) architecture is used. In such a case, the performances of both the chaotic and non-chaotic methods can be evaluated fairly on the same system. The details of the transmitter and the receiver for the proposed method are explained as follows.

A. *Transmitter*

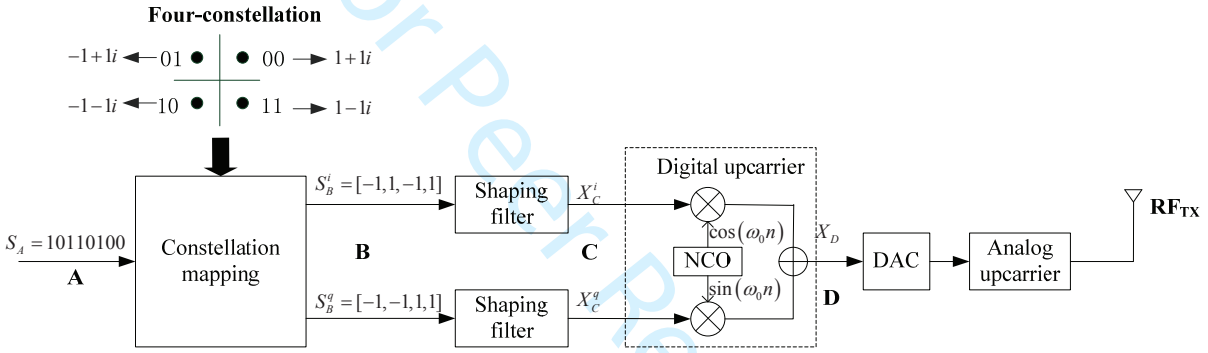

Fig. 1: Schematic diagram of the SDR transmitter

The schematic diagram of SDR transmitter is shown in Fig. 1. The signals at the ports A, B, C and D are represented as S_A, S_B, X_C and X_D, respectively. The original information S_A is a binary bit sequence, e.g., $S_A = [10110100]$. In general, there is no grammar constraint on the information, and '0' and '1' have equal probabilities. In modern digital communication, the binary information symbols are usually mapped into the predefined constellation diagram using constellation mapping, such as Multiple Phase Shift Keying (MPSK) and Multilevel Quadrature Amplitude Modulation (MQAM). After the constellation mapping, two signal sequences (in-phase signal S_B^i and quadrature signal S_B^q) are obtained at port B. In Fig. 1, an example of four-constellation QPSK mappings of S_A is shown, and the mapped signals $S_B^i = [-1, 1, -1, 1]$ and $S_B^q = [-1, -1, 1, 1]$.

The mapped signals, whose waveform are rectangular functions, cannot be transmitted directly because very large bandwidth is needed, which is not available. In practice, a shaping filter is used to convert the rectangular waveform to the baseband signal. The most commonly used filter in traditional communication is the raised cosine filter, which satisfies the Nyquist's ISI-free criterion. The most important distinction between our scheme and the traditional communication lies both in the baseband waveform and the corresponding shaping filter. In the following, the design of the shaping filter used in our method is described.

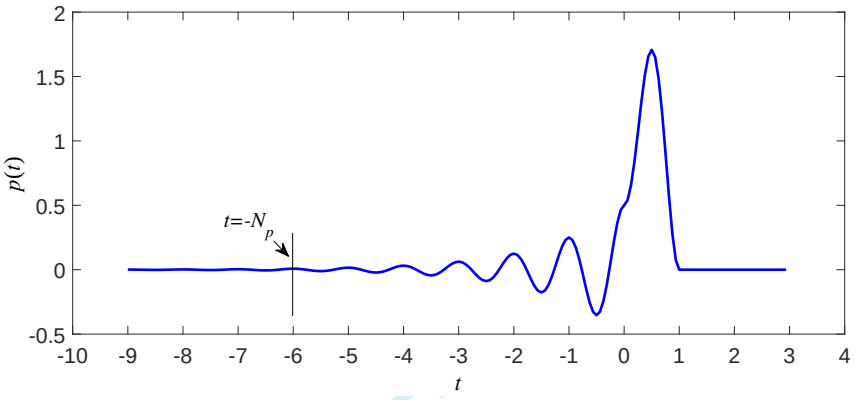

Fig. 2: The basis function $p(t)$ for $\beta = \ln 2$.

From the descriptions in Section II, we know that the chaotic waveform can be generated using linear superposition (2) of the basis function and the information symbol. In Eq. (2), an infinite symbol sequence is required for all $|t| < \infty$, this is infeasible in practical communication system. Figure 2 gives the basis function in Eq. (3) for $\beta = \ln 2$. It can be seen that $p(t) = 0$ when $t \geq 1$, then Eq. (2) can be approximately rewritten as

$$x(t) = \sum_{m=\lfloor t \rfloor}^{\lfloor t \rfloor + N_p} s_m \cdot p(t-m), \tag{7}$$

where $\lfloor t \rfloor$ indicates the largest integer less than or equal to t, and N_p is a positive integer satisfying $p(t) \approx 0$ for $t < -N_p$; Eq. (7) reveals that $x(t)$ only depends on the current and future N_p symbols. From Fig. (2), for $N_p = 6$ the requirement is satisfied. By this way, the shaping filter of the proposed method can be implemented by using the FIR filter. The block diagram of the FIR filter used to implement

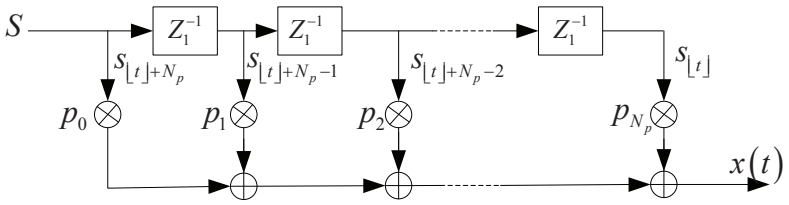

Fig. 3: FIR filter block diagram to implement the shaping filter.

the shaping filter is shown in Fig. 3, where symbol sequence S is the input signal. The unit delay, indicated by z_1^{-1}, is set as the symbol period of S, the taps number is N_p+1 and the taps coefficients $p_0, p_1, \cdots, p_{N_p}$ are determined by the basis function, given as

$$p_n = p(t - \lfloor t \rfloor - N_p + n), \qquad n = 0, 1, \cdots, N_p. \tag{8}$$

Usually, the sampling rate of the shaping filter output should be larger than the symbol rate of input signal. Assuming that the symbol rate at port B is r_B and the sampling rate at port C is r_C, we define

$$N_C = \frac{r_C}{r_B} \tag{9}$$

as the oversampling rate, and $N_C >= 2$. Then the sampling filtered signal at port C is

$$X_C = [x_C(0), x_C(1), x_C(2), \cdots], \tag{10}$$

where the nth element $x_C(n) = x(n/N_C)$.

When $N_C = 8$, the plots of symbol sequences, $S_B^i = [-1, 1, -1, 1]$ and $S_B^q = [-1, -1, 1, 1]$, at port B and their corresponding filter output (chaotic waveform), X_C^i and X_C^q, at port C are shown in Fig. 4. Because the symbol sequences and the chaotic waveform satisfy the topologically conjugate conditions as given in section II, we can retrieve the symbol sequences by sampling the filter output signal and comparing with a predetermined threshold.

After the shaping filter, a digital upcarrier is used to combine the in-phase and quadrature signals together, as shown in Fig. 1. The digital carrier signals, $\cos(\omega_0 n)$ and $\sin(\omega_0 n)$, are generated by the

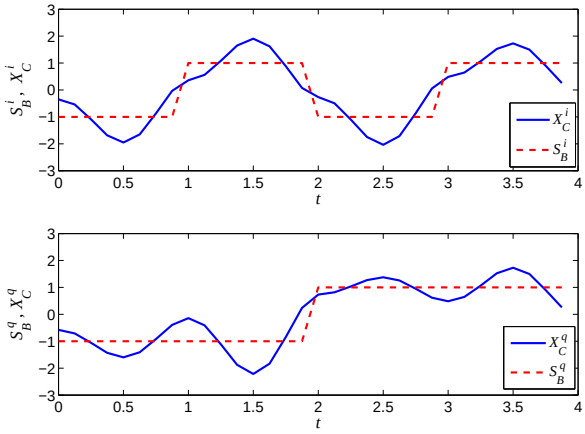

Fig. 4: The chaotic waveform using FIR filter ($N_C = 8$). The blue solid line on the upper panel is the in-phase shaping filter output signals, and the blue solid line on the lower panel is the quadrature shaping filter output signals.

Numerically Controlled Oscillator (NCO) given by

$$\begin{cases} \cos(\omega_0 n) = \cos(2\pi \dfrac{f_b}{f_s} n) \\ \sin(\omega_0 n) = \sin(2\pi \dfrac{f_b}{f_s} n) \end{cases}, \quad (n = 0, 1, 2, \cdots), \tag{11}$$

where f_b is the digital carrier frequency, and f_s is the sampling frequency of the digital carrier. In our scheme, we set f_s/f_b equal to the oversampling rate N_C given in Eq. (9), and the value of f_s is depended on the converting speed of Digital-to-Analog Convert (DAC). The signal at port D is

$$X_D = [x_D(0), x_D(1), x_D(2), \cdots], \tag{12}$$

where the nth element is given as $x_D(n) = x_C^i(n)\cos(\omega_0 n) + x_C^q(n)\sin(\omega_0 n)$, $x_C^i(n)$ and $x_C^q(n)$ are the in-phase and the quadrature signals at port C, respectively.

In wireless communication systems, a DAC is used to convert the digital signal to analog signal, and a analog upcarrier is used to shift the signal to a higher radio frequency, which is converted into the electromagnetic wave by the antenna $\mathrm{RF_{TX}}$ and transmitted over the wireless media.

It is worth noting that Fig. 1 is a general transmitter structure, which can be used for both the proposed chaotic system and the traditional non-chaotic system. The only difference between the two transmitters

is the shaping filter, but the other parts are exactly the same.

B. Receiver

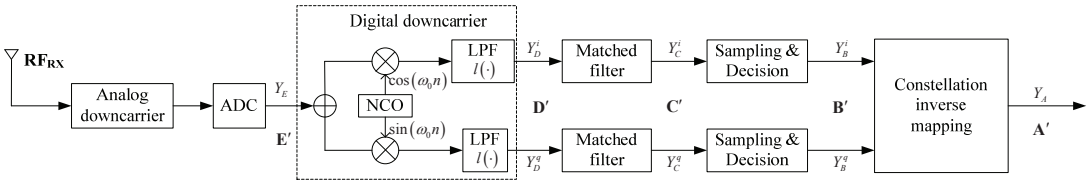

Fig. 5: Schematic diagram of the SDR receiver

The schematic diagram of SDR receiver is shown in Fig. 5, which is a reverse process of the transmitter in Fig. 1. The signals at the ports A′, B′, C′, D′ and E′ are represented as Y_A, Y_B, Y_C, Y_D and Y_E. After the wireless propagation, the analog RF signal received by antenna $\mathrm{RF_{RX}}$ is converted to digital signal by analog downcarrier and Analog-to-Digital Converter (ADC). Thus, $Y_E = [y_E(0), y_E(1), y_E(2), \cdots]$ is a sampling signal with the digital carrier frequency ω_0'. In order to detect the information symbols, the digital carrier should be removed to get the digital baseband signal. In Fig. 5, the digital downcarrier and the Low Pass Filter (LPF) are used to remove the digital carrier. Ideally, ω_0' is equal to the NCO's output frequency ω_0, and so the digital carrier can be removed completely. We assume that there is no frequency offset in the signal Y_E and that $l(\cdot)$ is the transfer function of LPF; the digital baseband (in-phase and quadrature) signals at port D′ are

$$\begin{cases} y_D^i(n) = l(y_E(n)\cos(\omega_0 n)) \\ y_D^q(n) = l(y_E(n)\sin(\omega_0 n)) \end{cases}, \qquad (n = 0, 1, 2, \cdots), \tag{13}$$

where $y_E(n)$ is the nth element of Y_E.

In noisy environment, a matched filter for a given waveform is the optimal linear filter for detecting the waveform [26]. For the chaotic waveform generated by Eq. (7), the matched filter can be realized by

$$y_C(t) = \sum_{m=\lceil t \rceil - N_C N_p}^{\lceil t \rceil} y_D(m) g(t-m), \tag{14}$$

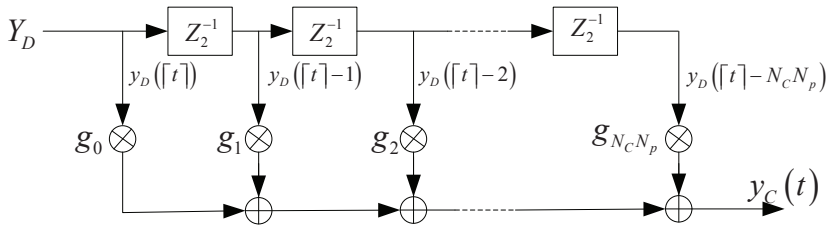

Fig. 6: FIR filter block diagram to implement the matched filter.

where $g(t) = p(-t)$ is a time-reversed basis function of $p(t)$, $\lceil t \rceil$ indicates the least integer larger than or equal to t. Equation (14) reveals that $y_C(t)$ depends on the current and past $N_C N_p$ samples (corresponding to N_p information symbols). Equation (14) can also be implemented by FIR filter structure given in Fig. 6.

It is worth noting that, the taps number and the unit delay, indicated by z_2^{-1}, in Fig. 6, are different from those in Fig. 3, this is because the symbol rates of the input signals in these two FIR filters are different. The taps number in Fig. 6 is $N_C N_p + 1$ and the taps coefficients $g_0, g_1, \cdots, g_{N_C N_p}$ are given by

$$g_m = g(t - \lceil t \rceil + m), \qquad m = 0, 1, \cdots, N_C N_p. \tag{15}$$

For detecting the symbols at the receiver, the symbol rates r_B at port B′ should be the same as that at port B in Fig. 1. By sampling $y_c(t)$ at rate r_B and comparing it with a preset threshold θ_n, the symbol corresponding to the nth sample can be decoded. We will give a detailed description about determining θ_n in the next Section. Finally, the binary symbol sequence can be retrieved by constellation inverse mapping.

In this Section, a wireless communication system using chaotic baseband waveform is designed in detail. Unlike the existing technologies [13] [16], which require high precision hardware and complex control algorithm to generate the chaotic waveform, the proposed method uses digital FIR filters to implement the chaotic shaping filter at the transmitter and uses the corresponding chaotic matched filter at the receiver. This is very important for the practical application of the proposed chaotic method because: 1) it can be implemented on the existing hardware, and without changing the transmitter/receiver structure; 2) the performance comparison with the traditional non-chaotic method can be done straightforwardly by using

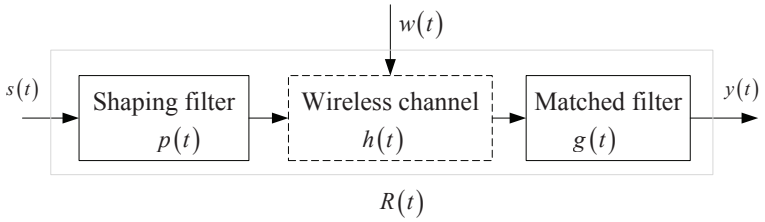

Fig. 7: Simplified block diagram of the wireless communication system using chaotic waveform.

the same hardware platform, and the comparison results are fair.

IV. Performance analysis of wireless communication using chaotic baseband waveform

In order to analyze the BER caused by ISI, a simplified block diagram (considering the baseband transmission only) of the proposed system is shown in Fig. 7, where $w(t)$ is an Additive White Gaussian Noise (AWGN). The main differences between our proposed system and the traditional system are the shaping filter and the corresponding matched filter. $p(t)$ and $g(t)$ are the impulse responses of the shaping filter and the matched filter, which are given by Eq. (2) and Eq. (14), respectively. The impulse response of the wireless multipath channel is given by

$$h(t) = \sum_{l=0}^{L-1} \alpha_l \delta(t - \tau_l), \tag{16}$$

where α_l and τ_l are the attenuation and propagation delay corresponding to path l from the transmitter to the receiver, and $\delta(\cdot)$ is the Dirac delta function. Assume that delay τ_l $(l = 0, 1, \ldots, L-1)$ satisfies $0 = \tau_0 < \tau_1 < \cdots < \tau_{L-1}$, then the channel fading α_l can be modeled as a negative exponential decay $\alpha_l = e^{-\gamma\tau_l}$, where γ is the damping coefficient. Equation (16) is a statistical average channel model [27] for a practical wireless communication channel, and it is considered for the theoretical performance analysis of the proposed method.

In Fig. 7, the total impulse response from the input to output can be described as

$$\begin{aligned} R(t) &= p(t) * h(t) * g(t) \\ &= p(t) * \Big(\sum_{l=0}^{L-1} \alpha_l \delta(t-\tau_l) \Big) * g(t) \\ &= \sum_{l=0}^{L-1} \alpha_l (p(t) * g(t)) * \delta(t-\tau_l) \\ &= \sum_{l=0}^{L-1} r(t-\tau_l) \end{aligned}, \tag{17}$$

where '*' denotes convolution and $r(t-\tau_l)$ can be calculated from Eq. (18), in which $A = \frac{(\omega^2-3\beta^2)}{4\beta(\omega^2+\beta^2)}$, $B = \frac{(3\omega^2-\beta^2)}{4\omega(\omega^2+\beta^2)}$ and $D = e^{-\beta|t-\tau_l|}$.

$$r(t-\tau_l) = \begin{cases} \alpha_l D(2-e^{-\beta}-e^{\beta})\big(A\cos\omega(t-\tau_l) + B\sin\omega(t-\tau_l)\big), & \text{if} \quad (|t-\tau_l| \geq 1) \\ \alpha_l \left\{ \begin{array}{l} A\big(D(2-e^{-\beta}) - D^{-1}e^{-\beta}\big)\cos\omega(t-\tau_l) + \\ B\big(D(2-e^{-\beta}) - D^{-1}e^{-\beta}\big)\sin\omega(t-\tau_l) + 1 - |t-\tau_l|, \end{array} \right\}, & \text{if} \quad (0 \leq |t-\tau_l| < 1) \end{cases} \tag{18}$$

The output signal $y(t)$ is

$$\begin{aligned} y(t) &= s(t) * R(t) + w(t) * g(t) \\ &= \sum_{m=-\infty}^{\infty} s(m) R(t-m) + W(t) \\ &= \sum_{l=0}^{L-1} \sum_{m=-\infty}^{\infty} s(m) r(t-m-\tau_l) + W(t) \end{aligned}, \tag{19}$$

where $s(m) \in \{-1, 1\}, m = -\infty, \cdots, \infty$ is a bi-polar symbol sequence, as given at port B in Fig. 1, with symbol rate r_B. $W(t) = w(t) * g(t)$ is the filtered noise. If $w(t)$ is an AWGN with zero mean, then $W(t)$ is also Gaussian noise with zero mean [28]. The output signal of the matched filter, $y(t)$, corresponds to the signal at port C′ in Fig. 5.

By sampling $y(t)$, using the interval $t = 1/r_B$ and recoding the nth sampling value as $y(n)$, we have

$$\begin{aligned} y(n) &= \sum_{l=0}^{L-1} \sum_{m=-\infty}^{\infty} s(m) r(n-m-\tau_l) + W(n) \\ &= \underbrace{s(n) \sum_{l=0}^{L-1} r(\tau_l)}_{Expected\ signal} + \underbrace{\sum_{\substack{m=\infty \\ m \neq n \\ m=-\infty}} s(m) \sum_{l=0}^{L-1} r(n-m-\tau_l)}_{Inter-symbol\ interference} + \underbrace{W(n)}_{Noise} \end{aligned} \tag{20}$$

In Eq. (20), the first term contains the expected symbol $s(n)$, the second term is the ISI from other symbol $s(m), m \neq n$. The values of $r(n-m-\tau_l)$ for different τ_l are plotted in Fig. 8. We can see that the ISI of chaotic communication system comes from two sources: Firstly, considering any one of the lines in Fig. 8, it shows that there exist several $n-m-\tau_l \neq 0$ such that $r(n-m-\tau_l) \neq 0$, which means that the communication signal using chaotic baseband waveform does not satisfy the Nyquist's ISI-free criterion [26], and there is an ISI even in the single path channel, although the ISI in the single path is small. Secondly, considering all of the three lines in Fig. 8, we have $r(n-m-\tau_l) \neq 0$ when $n-m-\tau_l = 0$, which means the ISI exists due to the multipath propagation.

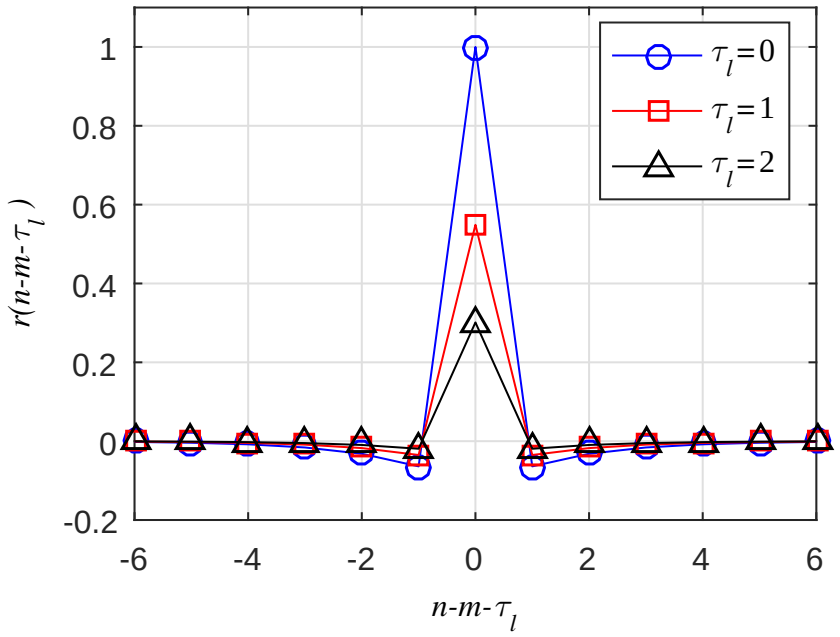

Fig. 8: ($\gamma = 0.6$) plots of $r(n-m-\tau_l)$ for different τ_l.

To detect the expected symbol, $s(n)$, from the sampled filtered signal, $y(n)$, a threshold θ_n is used to

decode the symbol as given by

$$s(n) = \begin{cases} 1, & \text{if } (y(n) \geq \theta_n) \\ -1, & \text{if } (y(n) < \theta_n) \end{cases}. \tag{21}$$

The intuitive threshold is $\theta_n = 0$, but a proper threshold can be designed to relief the ISIs from both aforementioned sources [23]. Under the multipath channel, the optimal threshold is

$$\theta_n^{opt} = \sum_{l=0}^{L-1} \sum_{\substack{m \neq n \\ m=-\infty}}^{m=\infty} s(m) r(n-m-\tau_l), \tag{22}$$

in which $r(n-m-\tau_l)$ can be calculated by using Eq. (18) if the channel parameters τ_l and α_l are known. Assuming that the variance of $W(n)$ is σ_W^2 and that $P = \sum_{l=0}^{L-1} r(\tau_l)$ is the total power of the expected symbol $s(n)$, BER using the optimal threshold, $\theta_n = \theta_n^{opt}$, is given as

$$p(\text{error}|\theta_n = \theta_n^{opt}) = \frac{1}{2} erfc\left(\frac{P}{\sqrt{2\sigma_W^2}}\right), \tag{23}$$

in which $erfc(\cdot)$ is the complementary error function. The optimal threshold θ_n^{opt} given in Eq. (22) contains both the past symbols $s(m)$ $(m < n)$ and the future symbols $s(m)$ $(m > n)$. At the current time, the past symbols have been decoded and it can be used for calculating θ_n^{opt}. However, in practice, the future symbols are unknown and θ_n^{opt} cannot be obtained using the available information. In this case, a suboptimal threshold, using only the past symbols, is given as

$$\theta_n^{subopt} = \sum_{\substack{m \neq n \\ m=-\infty}}^{m=\infty} s(m) \sum_{l=0}^{L-1} r(n-m-\tau_l). \tag{24}$$

Assume that the probability to send symbol "1" and "-1" is equal, i.e., $pr\big(s(m)=1\big) = pr\big(s(m)=-1\big) = 1/2$, where $pr(\cdot)$ is the probability of event '$\cdot$', then the BER using the suboptimal threshold $\theta_n = \theta_n^{subopt}$ is given as

$$\begin{aligned} &p(\text{error}|\theta_n = \theta_n^{subopt}) \\ &= \sqrt{2\sigma_W^2}\frac{e^{\beta}-1}{4|K|}\left\{ z_1 \cdot erfc(z_1) - z_2 \cdot erfc(z_2) - e^{-{z_1}^2}/\sqrt{\pi} + e^{-{z_2}^2}/\sqrt{\pi} \right\}, \end{aligned} \tag{25}$$

where $K = \sum_{l=0}^{L-1} \alpha_l (2 - e^{-\beta} - e^{\beta}) e^{-\beta\tau_l} \big(Acos(\omega\tau_l) + Bsin(\omega\tau_l)\big)$, $z_1 = \big(P + \frac{|K|}{e^{\beta}-1}\big)/\sqrt{2\sigma_W^2}$ and $z_2 = \big(P - \frac{|K|}{e^{\beta}-1}\big)/\sqrt{2\sigma_W^2}$.

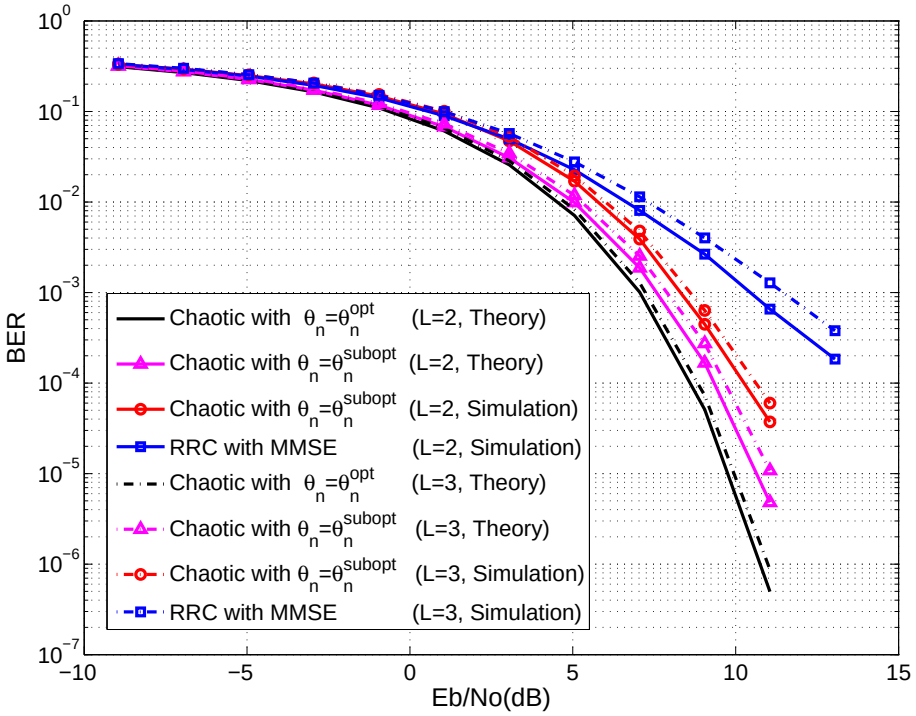

Fig. 9: (Static wireless channel) BER comparison results between wireless communication systems using the proposed chaotic and the conventional non-chaotic baseband waveform. The solid lines are the BER curves for the two-path channel (L=2) with $\tau_0 = 0$, $\tau_1 = 1$ and $\gamma = 0.6$, and the dash-dotted lines are the BER curves for the three-path channel (L=3) with $\tau_0 = 0$, $\tau_1 = 1$, $\tau_2 = 2$ and $\gamma = 0.6$. The lines without markers are the theoretical results using optimal threshold, the lines with upper triangular markers are the theoretical results using suboptimal threshold, the lines with circle markers are the simulation results using suboptimal threshold, and the lines with square markers are the simulation results using RRC and MMSE.

In the multipath channel (L=2 and L=3), the BER comparison results between wireless communication system using the proposed chaotic baseband waveform and the conventional non-chaotic baseband waveform are given in Fig. 9. For the wireless communication system using chaotic baseband waveform, the theoretical BER results from Eq. (23) and Eq. (25), and the simulation results using the suboptimal threshold $\theta_n = \theta_n^{subopt}$ are given in Fig. 9 as shown by the legend. For the wireless communication system

using non-chaotic baseband waveform, the commonly used Root Raised Cosine (RRC) shaping filter and the corresponding matched filter are used, at the same time, the Minimum Mean Square Error (MMSE) algorithm [29] is used for the channel equalization. During the simulation, the channel parameters, τ_l and γ, are invariant (static channel), and are known by the receiver. All the simulation results are obtained by averaging over 500 000 trials. Figure 9 shows that the wireless communication system using chaotic waveform and the optimal threshold has the lowest BER. The wireless communication system with the conventional RRC and MMSE has the worst BER. By using the suboptimal threshold, the BERs of chaotic waveform are not only lower than those of the conventional non-chaotic waveform, but also close (0.5dB gap for BER=10^{-3}) to the results using the optimal threshold. The simulation results using the suboptimal threshold is slightly worse than that of the corresponding theoretical results. This is because the retrieved past symbols are used in the calculation of the suboptimal threshold, and then the error decoding in the past affects the accuracy of the suboptimal threshold.

In the above analysis, the channel is static during the information transmission and the accurate channel parameters are known for symbol decoding. However, in practice, the wireless channel is time-varying and the channel parameters are unknown in advance. In such case, we consider the wireless channel as a time-varying but quasi-static channel, in which the channel parameters are assumed to be unchanged within one data frame, but are varied from one frame to the next. Figure 10 gives the BER comparison results under such a quasi-static channel. In our simulation, there are 4096 bits in one frame, which contains 256 training bits and 3840 information bits. The training bits are used for channel estimation using the least squares (LS) algorithm. The estimated channel parameters are used to calculate suboptimal threshold of our method and are used as parameters in the MMSE algorithm for the conventional non-chaotic system. The simulation results are obtained by averaging over 500 frames. In Fig. 10, BER simulation results of our wireless communication system using the proposed chaotic baseband waveform with the suboptimal threshold, the conventional non-chaotic waveform with RRC and MMSE, and the theoretical BER from Eq. (25) are given for comparison. We can see that the simulation BERs of both waveforms are worse than the corresponding results in Fig. 9, because of the imperfect channel estimation. However, for both

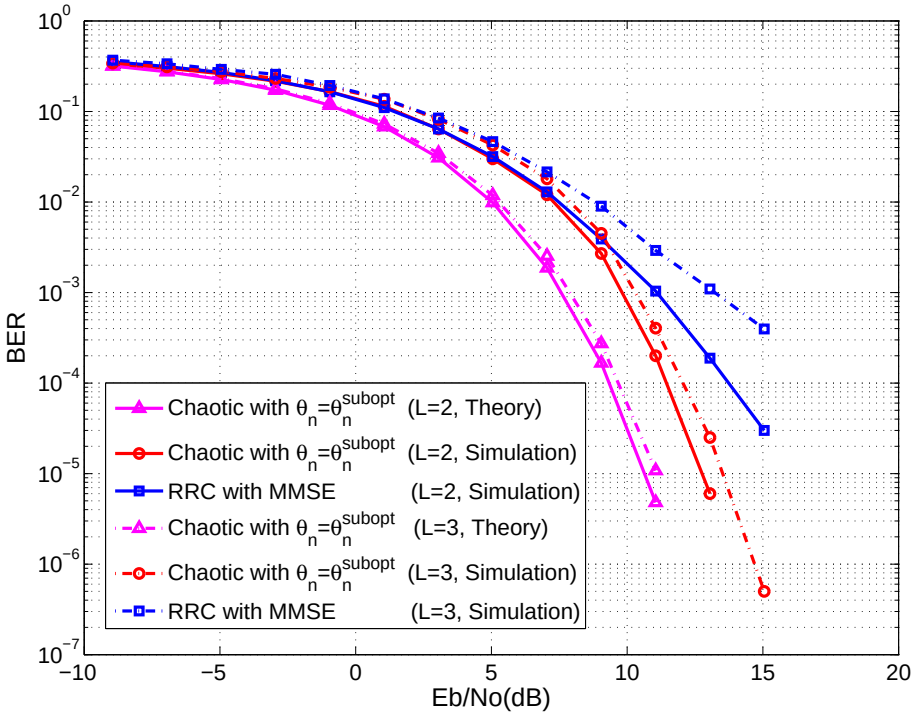

Fig. 10: (Time-varying wireless channel) BER comparison results between wireless communication system using the proposed chaotic and the conventional non-chaotic baseband waveform. The solid lines are the BER curves for the two-path channel (L=2), and the dash-dotted lines are the BER curves for the three-path channel (L=3). The lines with upper triangular markers are the theoretical results using suboptimal threshold, the lines with circle markers are the simulation results using suboptimal threshold, and the lines with square markers are the simulation results using RRC and MMSE.

two and three-path channels, the BER performance of the system using the chaotic baseband waveform is better than that of the conventional system using the non-chaotic baseband waveform.

V. Experimental Results

In order to demonstrate the practical performance of the proposed chaotic baseband waveform communication system, a radio-frequency wireless communication platform is used to realize both the chaotic and non-chaotic baseband waveforms.

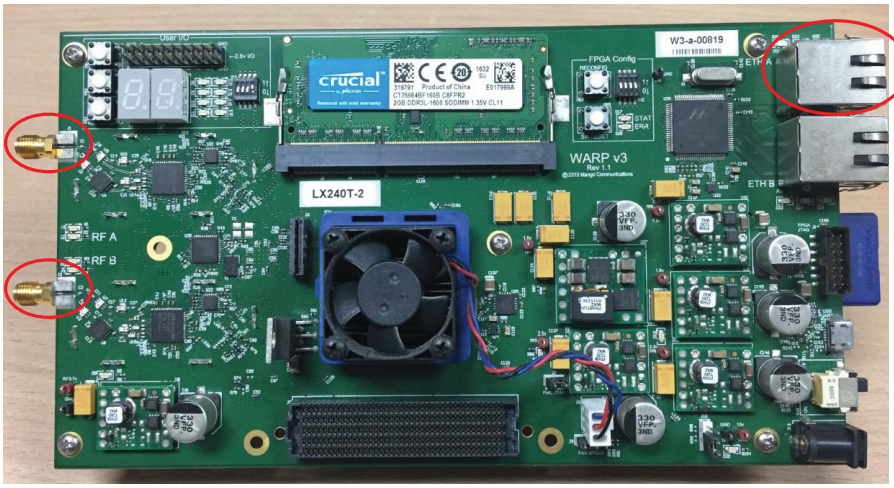

Fig. 11: Photo of the WARP node

The experiment is performed using wireless open-access research platform version 3 (WARP V3) designed by Rice University [30]. The hardware photo of the system is shown in Fig. 11, in the WAPR V3, the Xilinx Virtex-6 LX240T FPGA is used for digital signal processing, two MAX2829 RF chips are used to support dual-channel and 2.4GHz/5GHz dual-band transceiver, the maximum transmission power is 20dBm by using the dual-band power amplifier, the 12-bit low power analog/digital converter AD9963 is used to provide two ADC channels with sample rates of 100 MSPS and two DAC channels with sample rates of 170 MSPS, and two 10/100/1000 Ethernet interfaces (Marvell 88E1121R) can be used to realize the high-speed digital signal exchange with the Personal Computer (PC).

In order to validate the proposed chaotic based waveform for point-to-point communication based on the WARP, the WARPLab framework is used. The block diagram of WARPLab is shown in Fig. 12, in which two WARP nodes are connected with PC through 1Gbps Ethernet switch. Each WARP node has two radio antennas, which are referred as RFA and RFB. In our test, only the RFA, operating at the 2.4GHz carrier frequency with 20MHz bandwidth, in both nodes are used as transmitter (TX) and receiver (RX) for Single Input Single Output (SISO) communication.

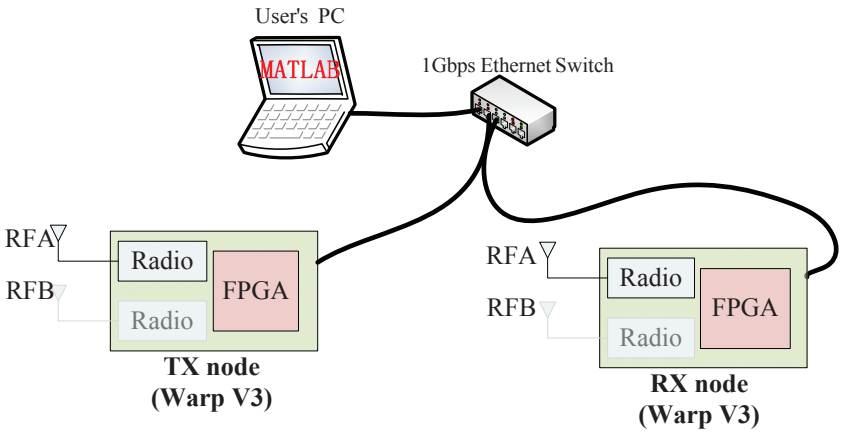

Fig. 12: Block diagram of WARPLab

In our experimental platform, the constellation mapping and the shaping filter are implemented on the PC using MATLAB R2016a, the digital upcarrier, DAC and the analog upcarrier are implemented on the WARP transmitter. After wireless propagation, the received RF signal is processed (through analog downcarrier, ADC and digital downcarrier) on the WARP receiver to obtain the complex received signal containing both the in-phase signal and the quadrature signal. The complex signal is then transferred to the PC for matching filtering and symbol detection in MATLAB environment. In this test, the data is transmitted frame by frame. There are 4096 bits in one frame, which contains 1023 training bits (using the Golden sequence) and 3073 data bits. The training bits in our experiment are not only used for channel estimation, but also for symbol synchronization and pilot-based frequency offset estimation.

A. The single path channel

At the outset, several basic properties of the experimental platform are tested in the laboratory, and the photo of the test scenario is given in Fig. 13(a). The chaotic baseband waveform is used and the transmission power is 3.5dBm in this test. After frequency offset calibration, the time domain waveform and the power spectrum of the received baseband signal are shown in Fig. 13(b) and Fig. 13(c), respectively. We can see from Fig. 13(c) that the 10dB bandwidth is about 8 MHz, thus the delay resolution of our experimental system is 0.125μs. The channel parameters, delay and fading, are

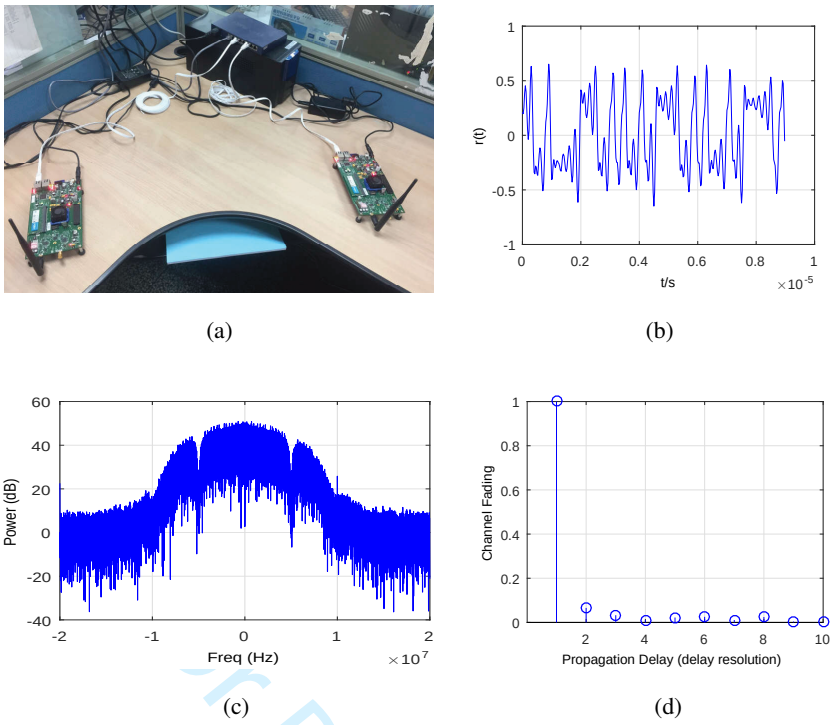

Fig. 13: (a) The photo of laboratory test, (b) the time domain waveform of received baseband signal, (c) the power spectrum of the received baseband signal, and (d) the normalized estimated channel parameters.

estimated by using the LS algorithm, and the normalized estimated channel parameters are shown in Fig. 13(d). We see that there is one main path with channel fading 1, and the other paths are relatively weak (i.e., the channel fading is less than 0.07). The unit of the x-axis in Fig. 13(d) is the delay resolution. The received baseband signal is filtered using the corresponding chaotic matched filter, and then the information symbol is decoded. In the laboratory environment, the symbols can be recovered without error. These results prove that the experimental platform can be used for RF wireless communication with chaotic baseband waveform.

B. The multipath channel

The BER performance of the proposed method under the real multipath channel is tested and, at the same time, the traditional method with the non-chaotic baseband waveform is also tested for comparison. In order to guarantee fairness of comparison, the transmission of both methods should be done as

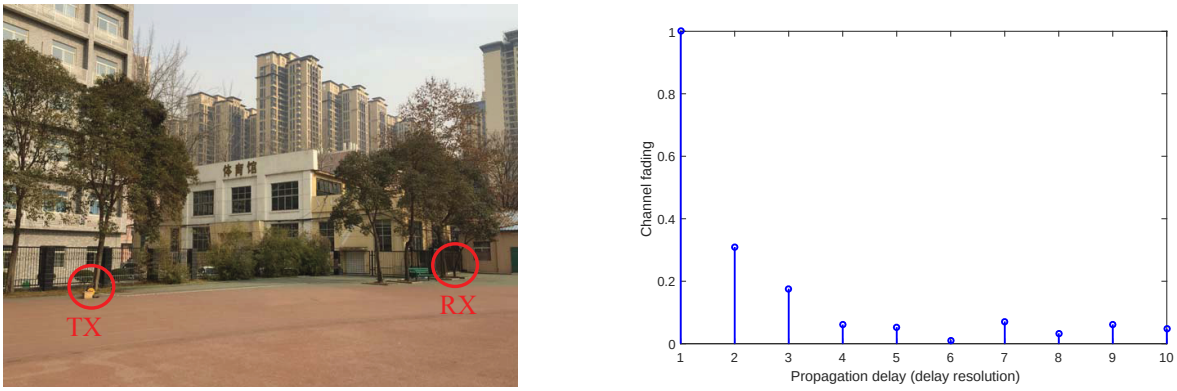

(a) (b)

Fig. 14: (a) The photo of the test in the first scenario, (b) the normalized estimated channel.

simultaneously as possible, because the channel may be time-varying. In the real environment, the channel coherence time is related to the speeds of terminals and clusters; we verify that the channel does not vary during the transmission of one frame in our test. Then, the 3073 data bits in one frame are divided into two parts, the first 1536 bits are using chaotic baseband waveform and the last 1537 bits are using non-chaotic baseband waveform. The channel parameters, estimated using the LS algorithm and 1023 training bits, are used for both methods. Two tests are carried out at the campus of our university, the first scenario is at the corner of the playground and the second scenario is in the middle of buildings. The experimental results are obtained by averaging over 100 frames.

The photo of the test in the first scenario is shown in Fig. 14(a). In this scenario, the distance between TX and RX is about 30 meters and there are some tall buildings in between. The channel parameters are estimated using the LS algorithm, and the normalized estimated channel parameters are shown in Fig. 14(b). We can see that there are three main paths with channel fading 1, 0.31 and 0.17, respectively. Because the delay resolution of our experimental system is 0.125μs, the delay of three paths are 0μs, 0.125μs and 0.25μs, respectively.

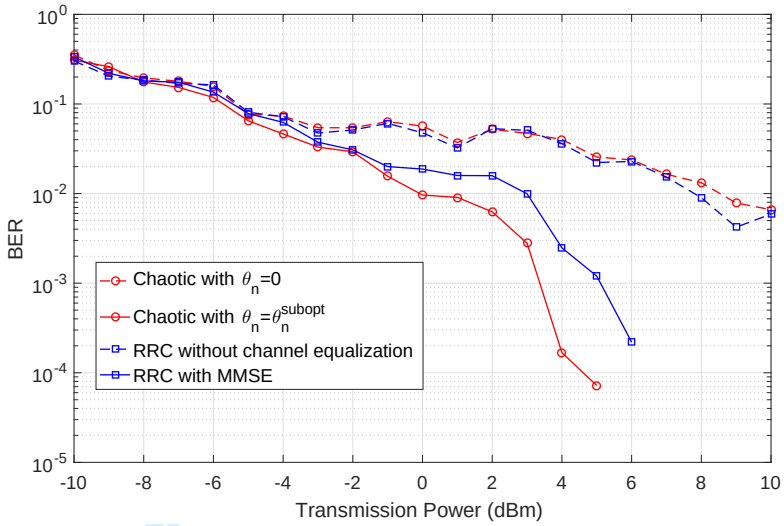

Fig. 15: The experimental BERs comparison in the first scenario

The BERs are tested for four methods: the proposed method using the chaotic baseband waveform and the suboptimal threshold, the proposed method using the chaotic baseband waveform and zero as threshold, the conventional method using RRC without channel equalization, and the conventional method using RRC and MMSE. In WARP V3, the transmission power can be adjusted by parameters TX_RF_Gain and TX_BB_Gain, and the maximum power is 20dBm. We adjust the transmission power to simulate the signal to noise ratio variation. The experimental BER varying with transmission power is shown in Fig. 15. We can see from Fig. 15 that the proposed chaotic baseband waveform using zero threshold and the conventional method without channel equalization have the worst BER among the four methods, because the ISIs are strong in these two cases. However, even with the suboptimal threshold, the performance improvement is significant for the chaotic baseband waveform. For BER=10^{-3}, the required transmission power is about 2dB lower than that of the conventional wireless communication system using RRC and MMSE.

The photo of the second test scenario is shown in Fig. 16(a), the distance between TX and RX is about 25 meters, there are some trees, cars and buildings in between, and there is not a line of sight between them. The normalized estimated channel parameters are shown in Fig. 16(b), there are four main paths with channel fading 1, 0.46, 0.19 and 0.21, respectively. The four methods in the first scenario

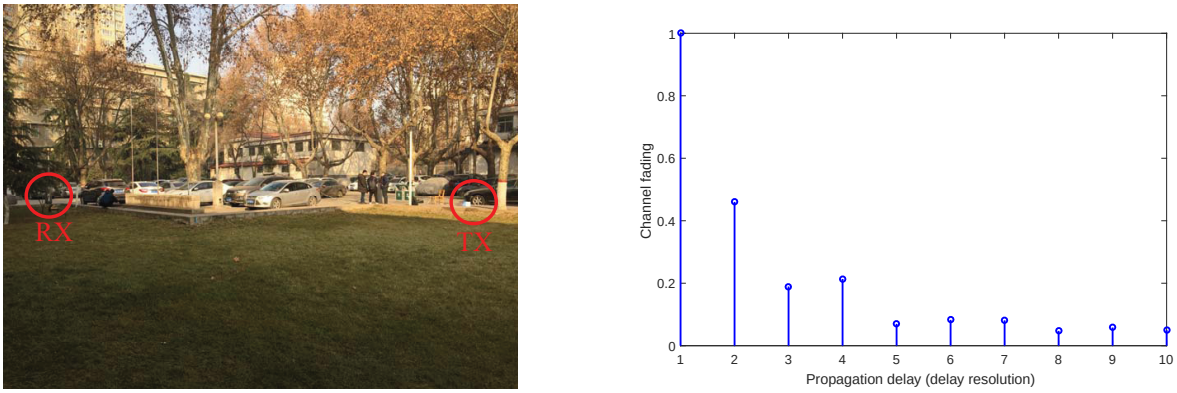

(a) (b)

Fig. 16: (a) The photo of the test in the second scenario, (b) the normalized estimated channel paramters.

are tested for comparison, and the experimental BERs versus the transmission power are shown in Fig. 17. We can see from Fig. 17 that the chaotic baseband waveform with suboptimal threshold has the best performance, the required transmission power for BER=10^{-3} is about 2.5dB lower than that of the conventional method using RRC and MMSE. The chaotic baseband waveform with zero as threshold and the conventional method without channel equalization have the worst BER, because the ISIs are not relieved in these cases.

Discussion 1. The proposed method needs the past symbols for calculating the suboptimal threshold. However, it's not necessary to use all of the past symbols, because $r(n-m-\tau_l)$ in Eq. (24) is close to zero for large enough $n-m-\tau_l$. In the implementation of our experiment, the past $5+\lceil\tau_{L-1}\rceil$ symbols are used to calculate the suboptimal threshold, where τ_{L-1} is the maximum channel delay. Initially, the training symbols are used to initialize our experimental system.

Discussion 2. Both the proposed method and the conventional method are implemented using the system configuration showing that our proposed method is compatible with the conventional system configuration, but achieving better BER performance.

Discussion 3. In addition, our proposed method is compatible with the conventional system configuration; the algorithm complexity of the proposed method is lower than the conventional method with MMSE because the threshold calculation is simple as compared to the MMSE algorithm.

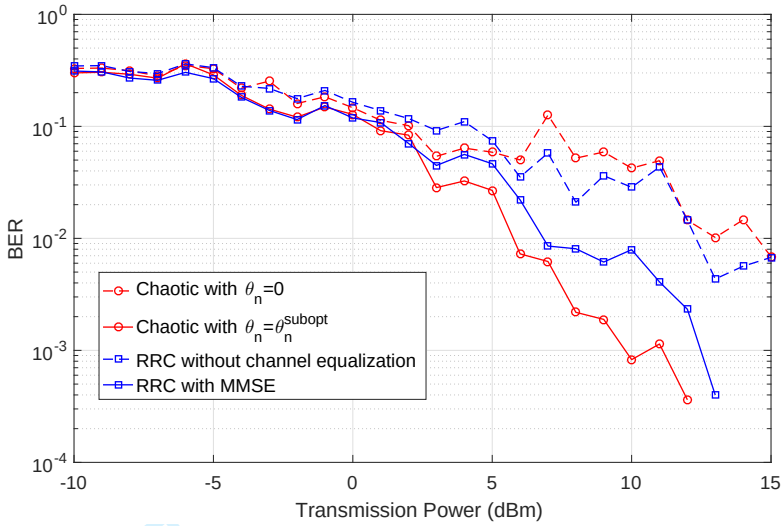

Fig. 17: The experimental BERs of three methods in the second scenario

VI. Conclusions

In this paper, a new idea of using chaos as wireless communication baseband waveform is proposed and our experimental results validate its effectiveness and superiority. In order to guarantee that the information can be retrieved from the received signal, a continuous-time chaotic waveform is shown to be topologically conjugate to the encoding symbolic dynamic (information). Based on this, a system structure of wireless communication using the chaotic baseband waveform is developed, in which the chaotic shaping filter and the corresponding matched filter are used to implement the encoding and maximize the SNR at the receiver. Under wireless multipath channel, the method in [23] is adopted to relieve the ISIs. The simulation comparison with the conventional wireless communication system shows that the proposed method has better performance under both the static and time-varying wireless channel. The experimental results show that, for BER=10^{-3}, the required transmiting power of the proposed method is 2dB$\sim$2.5dB lower than that of the conventional method. The merits of the wireless communication system using chaotic baseband waveform include that: i) the encoding method is simpler than the existing chaotic communication methods; ii) it is compatible with the common-used wireless communication equipment, and can be applied without changing the hardware of the existing digital wireless communication systems;

iii) it achieves lower BER than the conventional non-chaotic baseband waveform under wireless multipath channel. Thus, chaos-based wireless communication method proves to be a competitive alternative for a conventional wireless communication system.

REFERENCES

[1] C. Williams, "Chaotic communications over radio channels," *IEEE Transactions on Circuits and Systems I: Fundamental Theory and Applications*, vol. 48, no. 12, pp. 1394–1404, December 2001.

[2] Z. Li, K. Li, C. Wen, and Y. C. Soh, "A new chaotic secure communication system," *IEEE Transactions on Communications*, vol. 51, no. 8, pp. 1306–1312, August 2003.

[3] E. M. Bollt, "Review of chaos communication by feedback control of symbolic dynamics," *International Journal of Bifurcation and Chaos*, vol. 13, no. 02, pp. 269–285, February 2003.

[4] P. Chen, Y. Fang, K. Su, and G. Chen, "Design of a capacity-approaching chaos-based multi-access transmission system," *IEEE Transactions on Vehicular Technology*, vol. 66, no. 12, pp. 10 806–10 816, December 2017.

[5] K. M. Cuomo and A. V. Oppenheim, "Circuit implementation of synchronized chaos with applications to communications," *Physical Review Letters*, vol. 71, no. 1, pp. 65–68, July 1993.

[6] F. C. M. Lau and C. K. Tse, *Chaos-Based Digital Communication Systems*. Springer Berlin Heidelberg, 2003.

[7] H. Yang, W. K. S. Tang, G. Chen, and G. P. Jiang, "Multi-carrier chaos shift keying: System design and performance analysis," *IEEE Transactions on Circuits and Systems I: Regular Papers*, vol. 64, no. 8, pp. 2182–2194, August 2017.

[8] A. P. Kurian, S. Puthusserypady, and M. H. Su, "Performance enhancement of ds/cdma system using chaotic complex spreading sequence," *IEEE Transactions on Wireless Communications*, vol. 4, no. 3, pp. 984–989, May 2005.

[9] G. Kolumban, B. Vizvari, W. Schwarz, and A. Abel, "Differential chaos shift keying: A robust coding for chaos communication," in *IEEE International Workshop on Nonlinear Dynamics of Electronic Systems*, Seville, Spain, January 1996, pp. 92–97.

[10] M. P. Kennedy, G. Kolumban, G. Kis, and Z. Jako, "Performance evaluation of fm-dcsk modulation in multipath environments," *IEEE Transactions on Circuits and Systems I: Fundamental Theory and Applications*, vol. 47, no. 12, pp. 1702–1711, December 2000.

[11] G. Kaddoum, "Wireless chaos-based communication systems: A comprehensive survey," *IEEE Access*, vol. 4, pp. 2621–2648, May 2016.

[12] W. Xu, T. Huang, and L. Wang, "Code-shifted differential chaos shift keying with code index modulation for high data rate transmission," *IEEE Transactions on Communications*, vol. 65, no. 10, pp. 4285–4294, October 2017.

[13] S. Hayes, C. Grebogi, and E. Ott, "Communicating with chaos," *Phys. Rev. Lett.*, vol. 70, pp. 3031–3034, May 1993.

[14] E. Rosa, S. Hayes, and C. Grebogi, "Noise filtering in communication with chaos," *Phys. Rev. Lett.*, vol. 78, pp. 1247–1250, February 1997.

[15] T. L. Carroll and F. J. Rachford, "Chaotic sequences for noisy environments," *Chaos An Interdisciplinary Journal of Nonlinear Science*, vol. 26, no. 10, pp. 927–936, October 2016.

[16] H. P. Ren, C. Bai, J. Liu, M. S. Baptista, and C. Grebogi, "Experimental validation of wireless communication with chaos," *Chaos*, vol. 26, no. 8, p. 083117, August 2016.

[17] H. P. Ren, M. S. Baptista, and C. Grebogi, "Wireless communication with chaos," *Phys. Rev. Lett.*, vol. 110, p. 184101, May 2013.

[18] L. M. Pecora and T. L. Carroll, "Synchronization in chaotic systems," *Physical Review Letters*, vol. 64, no. 8, pp. 821–824, February 1990.

[19] A. Argyris, D. Syvridis, L. Larger, V. Annovazzi-Lodi, P. Colet, I. Fischer, J. Garcia-Ojalvo, C. R. Mirasso, L. Pesquera, and K. A. Shore, "Chaos-based communications at high bit rates using commercial fibre-optic links," *Nature*, vol. 438, pp. 343 – 346, November 2005.

[20] S. T. Hayes, "Chaos from linear systems: implications for communicating with chaos, and the nature of determinism and randomness," *Journal of Physics: Conference Series 23*, pp. 215–237, January 2005.

[21] Y. Hirata and K. Judd, "Constructing dynamical systems with specified symbolic dynamics," *Chaos An Interdisciplinary Journal of Nonlinear Science*, vol. 15, no. 3, p. 33102, September 2005.

[22] N. J. Corron, J. N. Blakely, and M. T. Stahl, "A matched filter for chaos," *Chaos*, vol. 20, no. 2, p. 023123, June 2010.

[23] J. Yao, C. Li, H. Ren, and C. Grebogi, "Chaos-based wireless communication resisting multipath effects," *Physical Review E*, vol. 96, p. 032226, September 2017.

[24] L. Zhu, Y. C. Lai, F. C. Hoppensteadt, and E. M. Bollt, "Numerical and experimental investigation of the effect of filtering on chaotic symbolic dynamics," *Chaos*, vol. 13, no. 1, pp. 410–419, March 2003.

[25] H. P. Ren, W. Y. Zheng, and C. Grebogi, "Radio-wave communication with chaos," *Chinese Physics B*, to appear.

[26] J. G. Proakis and M. Salehi, *Digital Communication, Fifth Edition*. McGraw-Hill Higher Education, New York, 2008.

[27] J. Meinila, P. Kysti, T. Jamsa, and L. Hentila, "Winner ii channel models," in *Radio Technologies and Concepts for IMT-Advanced*. John Wiley Sons, Ltd., New York, 2009, pp. 39–92.

[28] J. N. Blakely, D. W. Hahs, and N. J. Corron, "Communication waveform properties of an exact folded-band chaotic oscillator," *Physica D Nonlinear Phenomena*, vol. 263, no. 22, pp. 99–106, November 2013.

[29] M. Tuchler, A. C. Singer, and R. Koetter, "Minimum mean squared error equalization using a priori information," *IEEE Transactions on Signal Processing*, vol. 50, no. 3, pp. 673–683, Mar 2002.

[30] "Wireless open access research platform," http://warp.rice.edu.